Journal of Structural Geology, Vol. 7, No. 2, pp. 187 to 203, 1985
Printed in Great Britain

0191-8141/85 $03.00 + 0.00

Dynamothermal transition zone between Archaean greenstone and granitoid gneiss at Lake Dundas, Western Australia

JOHN G. SPRAY

Department of Earth Sciences, University of Cambridge, Cambridge, CB2 3EQ, U.K.

(*Received* 16 *April* 1984; *accepted in revised form* 13 *September* 1984)

Abstract—A 500 m wide shear zone occurs between the base of an Archaean greenstone sequence and adjacent granitoid gneiss complex on the shores of Lake Dundas, Western Australia. The dynamothermal margin remains distinguishable due to the preservation of upper amphibolite facies assemblages, related granitoid anatectites and mylonitic, schistose and gneissose fabrics developed parallel to the contact, which itself lies subparallel to the greenstone bedding surface. The margin contrasts with less deformed greenschist to low amphibolite facies assemblages which characterize lithologies within the greenstone belt, many of which retain igneous textures and relict primary phases. Structural, petrological and textural evidence indicates that the dynamothermal contact originally evolved as a subhorizontal ductile shear zone during juxtaposition of the greenstone pile with granitoid gneiss and that its formation preceded regional folding, greenschist facies overprinting and granitoid intrusion which occurred at about 2700 Ma. The amount of heat generated within the transition zone during thrusting was limited to maximum temperatures of *c.* 650°C due to the buffering effect of granitoid anatexis.

INTRODUCTION

THE RELATIONSHIP between Archaean greenstone and granitoid gneiss terrains remains controversial. Debate centres on the nature of the basement to the greenstones and whether, if originally granitoid, it can be distinguished from younger granitoid material which itself may have undergone several phases of deformation and metamorphism. The style and controls of metamorphism within greenstone sequences are also poorly understood. Many sequences show pronounced changes in grade and deformation intensity within relatively short distances ($\ll$1 km) and in this respect appear to differ from the style of regional metamorphism more typical of Proterozoic and Phanerozoic terrains. For example, in many Archaean greenstone belts low to medium grade 'static' domains showing recrystallization without deformation can be contrasted with medium to high grade 'dynamic' domains showing both recrystallization and deformation (e.g. Binns *et al.* 1976). The dynamic or sheared domains usually occur along the edges of the greenstone sequences and the static domains occur within them. This relationship is characteristic of many greenstone areas within the Eastern Yilgarn Block of Western Australia and it is from here that a particular 'dynamic' domain at the margin of a greenstone sequence through to adjacent granitoid gneiss is described and its probable origins discussed. This work is specifically concerned with the field and structural relations between granitoid gneiss and greenstones exposed on the shore of Lake Dundas. The selected area is a crucial one as it is located at the southern end of the vast linear Norseman–Wiluna greenstone belt where the deeper levels of greenstone stratigraphy and contact relations with polydeformed granitoid gneiss are exposed. Potentially the study area may therefore provide insight into the early structural relations of this granitoid–greenstone terrain.

REGIONAL GEOLOGY

Lake Dundas is a large playa situated about 200 km S of Kalgoorlie and 20 km S of Norseman on the SE margin of the Archaean Yilgarn Block, Western Australia. It occurs within an area of subdued topography and poor exposure with the exception of the western flanks of salt lakes which provide good outcrop. Geologically the area forms part of the *c.* 700 km long granitoid–greenstone terrain of the Eastern Goldfields Province (Fig. 1)(Doepel 1973, Gemuts & Theron 1975, Gee *et al.* 1981).

The region comprises a polydeformed granitoid gneiss terrain surrounding a metamorphosed volcano-sedimentary complex (the greenstone supracrustal sequence) within which occur deformed and undeformed granitoid bodies. The greenstone sequence consists of four distinct stratigraphic units: the Penneshaw, Noganyer, Woolyeenyer and Mount Kirk Formations which together attain a maximum apparent thickness of *c.* 24 km N of Norseman (Fig. 2)(Sofoulis 1963, Hall & Bekker 1965, Doepel 1973). They consist of metamorphosed pillow lavas, basaltic and ultrabasic flows, doleritic and gabbroic sills and dykes and metasedimentary intercalations (including metamorphosed banded iron formation, shales, siltstones, sandstones, conglomerates and pyroclastics). Sills and dykes of felsite are also common in the higher stratigraphic units. The Penneshaw and Woolyeenyer Formations are predominantly basic to ultrabasic while the Noganyer and Mount Kirk Formations contain appreciable amounts of sediment. Wherever pillow lava facings and various sedimentary structures can be observed they indicate that the greenstone sequence youngs from the Penneshaw through to the Mount Kirk Formation, although it should be emphasized that our stratigraphic knowledge of the Norseman greenstones is still poor, especially outside areas of immediate economic interest. Structural

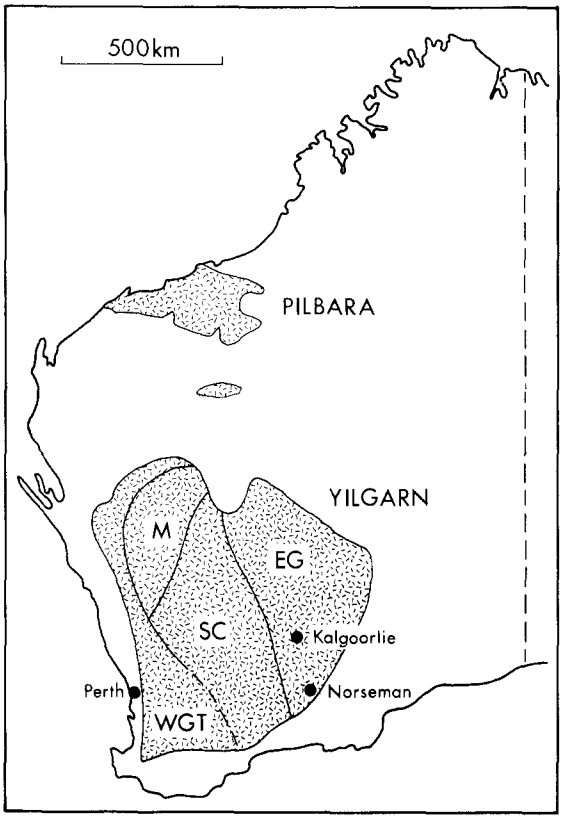

Fig. 1. Archaean cratons of Western Australia showing regional subdivisions of the Yilgarn Block after Gee *et al.* (1981). EG, Eastern Goldfields Province; SC, Southern Cross Province; M, Murchison Province; WGT, Western Gneiss Terrain.

breaks and repetition have not been proven within the greenstone sequence, but previous workers have noted the presence of drag folds (Ellis 1953) and the likelihood of stratigraphic discontinuities occurring within the Noganyer Formation (Doepel 1973).

During the present project four main episodes of Archaean deformation ($D1$–$D4$) were recognized within the greenstones and some of the metamorphic granitoids. Certain metamorphic granitoids also show evidence of pre-$D1$ deformation not identified in the greenstones (discussed later). The youngest of the four deformation episodes (here designated $D4$) comprises a subvertical, ENE-trending fracture cleavage ($S4$) with associated upright open folds ($F4$). $D3$ is the main regional deformation event and resulted in the formation of a steep NNW-trending schistosity ($S3$) which is axial planar to $F3$ folds. The greenstone sequence is steeply dipping and asymmetrically disposed about one of the larger $F3$ folds: the Norseman Anticline. Its western limb extends SSW for over 50 km, while the eastern limb is only locally preserved for about 20 km as SE-trending lenses and narrow discontinuous bands. Together the $F4$ and $F3$ folds intersect to create an egg-box interference pattern, the domes of which often coincide with granitoid diapirs. A number of large transcurrent faults are also considered to have been active (or reactivated) during $D3$ (Gee 1979, Gee *et al.* 1981). These NNW-trending lineaments occur throughout the Eastern Goldfields Province and commonly border the greenstone sequences. $D2$ created the Mount Kirk Syncline and Penneshaw Anticline which are themselves folded about the main $F3$ axis (Fig. 2). $D1$ is the earliest greenstone event recorded and is of a localized nature, being restricted to the transition between greenstones and granitoid gneiss in the form of a shear zone. Steeply dipping mylonitic, schistose and gneissose fabrics ($S1$) containing intrafolial folds ($F1$) are developed over a distance of up to 500 m about these contracts.

Peak regional metamorphism reached the greenschist to lower amphibolite facies and was coincident with the $D3$ event. Higher grades, up to amphibolite facies, were locally realized around granitoid diapirs (such as the Pioneer and Goodia Domes), undeformed post-tectonic granitoids and at sheared greenstone margins in contact with polydeformed granitoid gneiss. The structural scheme presented is similar, though not identical, to that proposed for the Kambalda (Gresham & Loftus-Hills 1981) and Widgiemooltha–Pioneer (Archibald *et al.* 1978) areas N of Norseman.

AGE CONSTRAINTS

Relatively few radiometric age data are currently available for the Archaean granitoids and greenstones within the area covered by Fig. 2. The exceptions are the results of Turek (1966), Oversby (1975) and McCulloch *et al.* (1983). Turek (1966) reported Rb–Sr data for various lithologies within the greenstone sequence and concluded (op. cit. p. 64) that Archaean sedimentation and volcanism in the Kalgoorlie–Norseman area was terminated by a regional metamorphic and metasomatic event at 2665 ± 25 Ma. This is in good agreement with the timing of greenschist facies metamorphism dated at 2610 ± 30 Ma by a Rb–Sr isochron on the footwall and hanging-wall metabasalts at Kambalda 160 km of Norseman (Roddick 1984). Oversby (1975) obtained Pb–Pb mineral isochrons from granitoids of 2617 ± 79 Ma for Stennet Rocks and 2655 ± 35 Ma for Buldania Rocks (see Fig. 2 for locations) and inferred that their crustal development history spanned at least 700 Ma (i.e. from about 3300 to 2600 Ma). Establishing the primary ages of the granitoid gneisses and greenstones has proven both difficult and contentious. McCulloch *et al.* (1983) have recently obtained Rb–Sr and Sm–Nd whole-rock ages of 2780 ± 60 Ma and 2800 ± 100 Ma respectively for granitoid gneiss sampled from a supposed 'basement' inclusion within the Pioneer Dome (Archibald & Bettenay 1977). This is in close agreement with a Sm–Nd age of 2790 ± 30 Ma for mafic–ultramafic and felsic volcanics from the Kambalda greenstones (McCulloch & Compston 1981). Also from Kambalda, but in contrast to these results, Claoue-Long *et al.* (1984) report a Sm–Nd whole-rock isochron age of 3262 ± 44 Ma for ultramafic–mafic lavas from the Kambalda and Bluebush sequences. However, it is not the purpose of this paper to discuss the respective merits of the different supposed primary ages obtained from the Kambalda greenstone sequence, nor whether genuine granitoid gneiss 'basement' has been

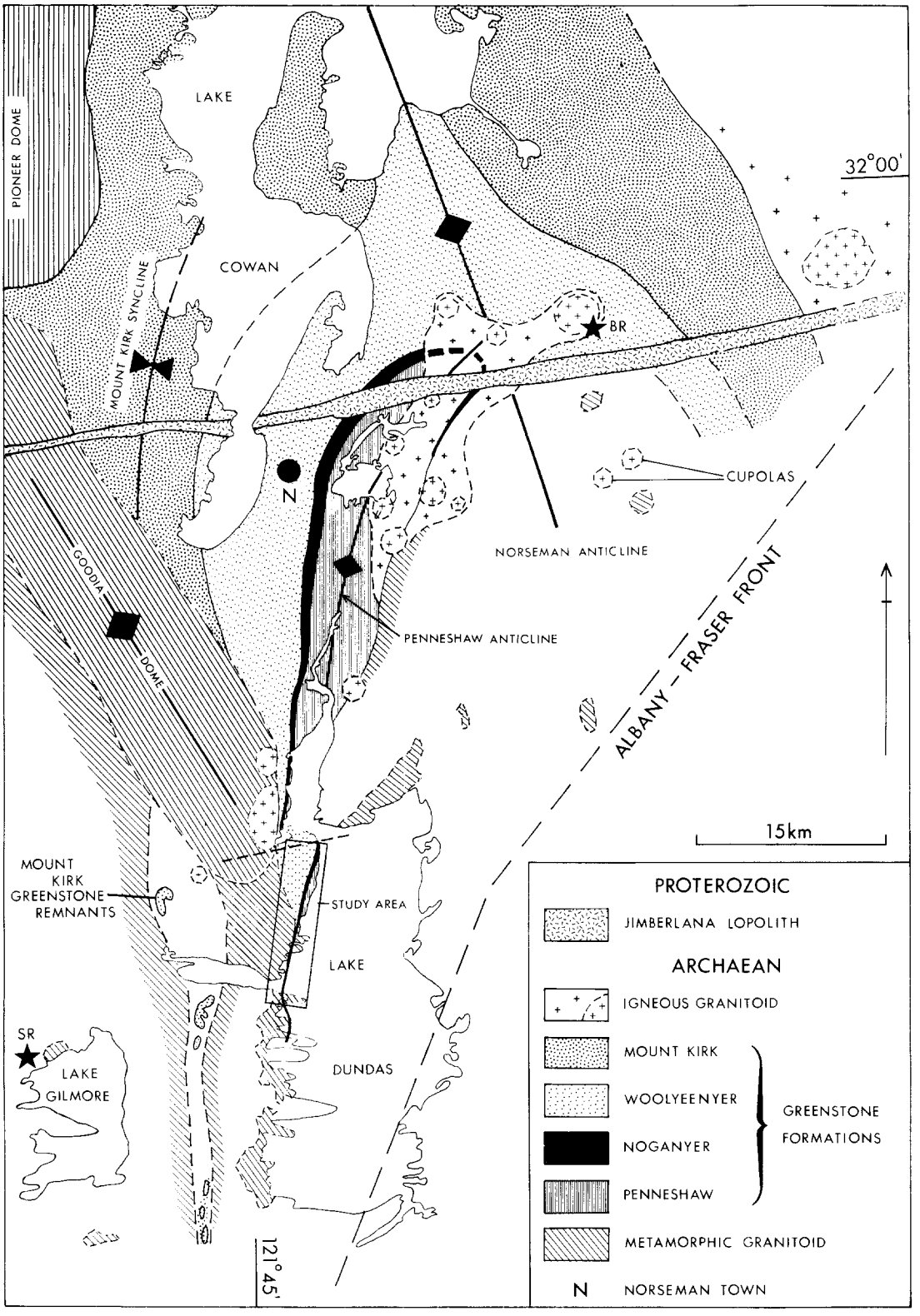

Fig. 2. Simplified geology of the Norseman region showing greenstone stratigraphy and location of transition zone study area. Metamorphic granitoids possess some form of deformation fabric or evidence of subsolidus recrystallization. Black stars indicate the locations of granitoids dated by Oversby (1975). SR, Stennet Rocks; BR, Buldania Rocks. The study area (Fig. 4) is outlined.

dated at the Pioneer Dome. A greater consensus exists regarding the timing of late Archaean regional greenschist facies metamorphism which appears to have largely reset Rb–Sr ages throughout the Eastern Goldfields Province. This age approximates 2700 Ma (Turek 1966, Roddick 1984) and coincides with a period of granitoid remobilization (Oversby 1975) and regional deformation (Binns *et al.* 1976). In this work the *c.* 2700 Ma event is used as a reference point for the four deformation episodes recognized within the Norseman region. The *D*2, *D*3 and *D*4 events are taken to constitute the *c.* 2700 Ma regional tectonometamorphic

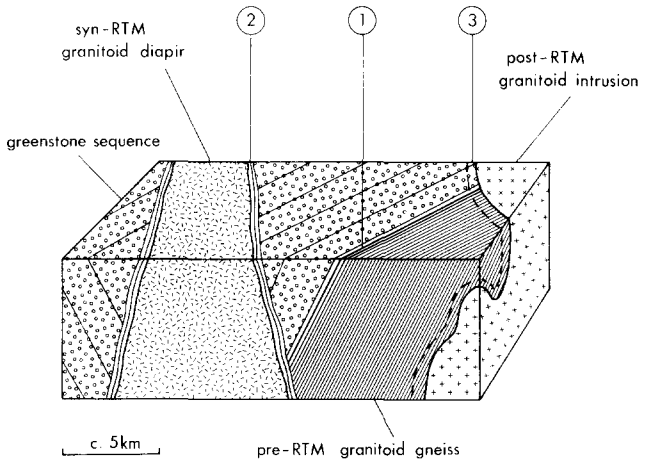

Fig. 3. Schematic representation of the three types of granitoid–greenstone contact distinguished in the Norseman region. 1, concordant shear zone between pre-regional tectonometamorphic (pre-RTM) granitoid and greenstone developed subparallel to greenstone bedding surface; 2, discordant syn-RTM granitoid gneiss diapir intruded into greenstone synform with strained aureole; 3, discordant post-RTM igneous granitoid with unstrained aureole.

episode, the peak of which coincided with *D*3. *D*2–*D*4 are thus referred to as syn-RTM (Regional TectonoMetamorphic) while pre-RTM refers to events prior to *D*2 and post-RTM to events after *D*4.

With regard to the timing of post-Archaean events, the granitoid–greenstone terrain is intruded by an Early Proterozoic group of predominantly ENE-trending basic dykes known as the Widgiemooltha Dyke Suite. The largest of these is the Jimberlana lopolith situated 5 km N of Norseman (Campbell *et al.* 1979) dated at about 2400 Ma (Turek 1966). Approximately 30 km to the E and SE of Lake Dundas the Yilgarn Block is bordered by the Mid-Proterozoic Albany–Fraser Complex which reaches granulite facies grade and shows evidence of migmatization and granitoid intrusion spanning 1900 to 1200 Ma (Compston & Arriens 1968, Arriens & Lambert 1969, Lovering *et al.* 1981).

THE GREENSTONE–GRANITOID GNEISS TRANSITION ZONE

Occurrence and general geology

Three fundamentally distinct types of granitoid–greenstone contact are recognized in the Norseman region and these are referred to as pre-, syn- and post-RTM. For simplicity the contacts are classified, like the deformation episodes, relative to the *c.* 2700 Ma late Archaean regional tectonometamorphic episode (*D*2–*D*4). Their distinction is crucial if the structural and metamorphic evolution of the greenstones is to be understood even at a simple level (Fig. 3).

Pre-RTM contacts show the most complex structures and are exposed at several localities in the Norseman region. One of the most extensive outcrops occurs along the western shore of Lake Dundas where a study area of *c.* 50 km^2 was mapped over a period of about three months using aerial photographs enlarged to 1:7500 scale (Figs. 2 and 4). Other examples include the Penneshaw greenstone–granitoid gneiss contact 10 km SSE of Norseman (as revealed by seven Central Norseman Gold Corporation diamond drill cores: PE1–7), the adjacent region E of Waratah and the Albion–Gilmore–Beete greenstone remnants of the Mount Kirk Formation located between Lakes Dundas and Gilmore (Fig. 2). All are characterized by highly sheared contacts up to 500 m wide comprising fine to medium grained schistose amphibolites juxtaposed and interleaved with granitoid gneiss (Fig. 5). The contact zone attains upper amphibolite facies grade and characteristically occurs subparallel to greenstone bedding surfaces. This type of contact contrasts with syn-RTM and post-RTM granitoid–greenstone junctions. Syn-RTM granitoids are discordantly intrusive into the greenstone pile, cutting across greenstone bedding surfaces and *D*1 and *D*2 structures. They are metamorphically recrystallized with an *S*3 (NNW) fabric predominant, frequently possess trends coaxial to *F*3 axial surfaces (e.g. a *D*3 gneiss dome truncates the Mount Kirk *F*2 Syncline, Fig. 2) and generally form large elongate bodies with strained amphibolite facies aureoles (e.g. the Pioneer and Goodia Domes, Fig. 2). Post-RTM (post-*D*4) granitoids show no evidence of metamorphic recrystallization and retain igneous textures. They too are discordantly intrusive into the greenstone pile but possess static amphibolite facies aureoles. They typically occur as ovoid stocks up to a few km diameter (e.g. 10 km E of Norseman, Fig. 2). Both syn- and post-RTM granitoids contain rounded xenoliths of metabasites (amphibolites) presumably derived by stoping and wedging into the greenstones. Syn- and post-RTM granitoid–greenstone contacts will be discussed in more detail elsewhere. In this work it is the pre-RTM contact structural relations which are considered.

Preliminary XRF geochemical data obtained from over sixty granitoid samples from the Norseman area reveal the existence of two major compositional suites: granite (*sensu stricto*) and trondhjemite–tonalite. A large ovoid trondhjemite–tonalite 'dome' occupies the region E of Norseman and S of the Jimberlana lopolith. The remaining area is dominated by granite *s.s.* Little correlation is found to exist between tectonic style and granitoid chemistry: remobilized syn- or post-RTM granitoids appear to possess compositions similar to surrounding pre-RTM gneisses. However, further geochemical work is in progress to investigate these apparent differences more fully.

The study area covers part of the western limb of the Penneshaw Anticline immediately S of an ENE-trending sinistral wrench fault which has displaced the greenstone sequence 3 km to the E (Fig. 4). Owing to the subvertical dip of the greenstone sequence, Fig. 4 essentially shows a cross-section with granitoids to the E and W and the basal Penneshaw, middle Noganyer and overlying Woolyeenyer Formations of the greenstone sequence in the centre. Granitoids to the W are of a varied nature and include pre-RTM gneisses and a syn-RTM (*D*3)

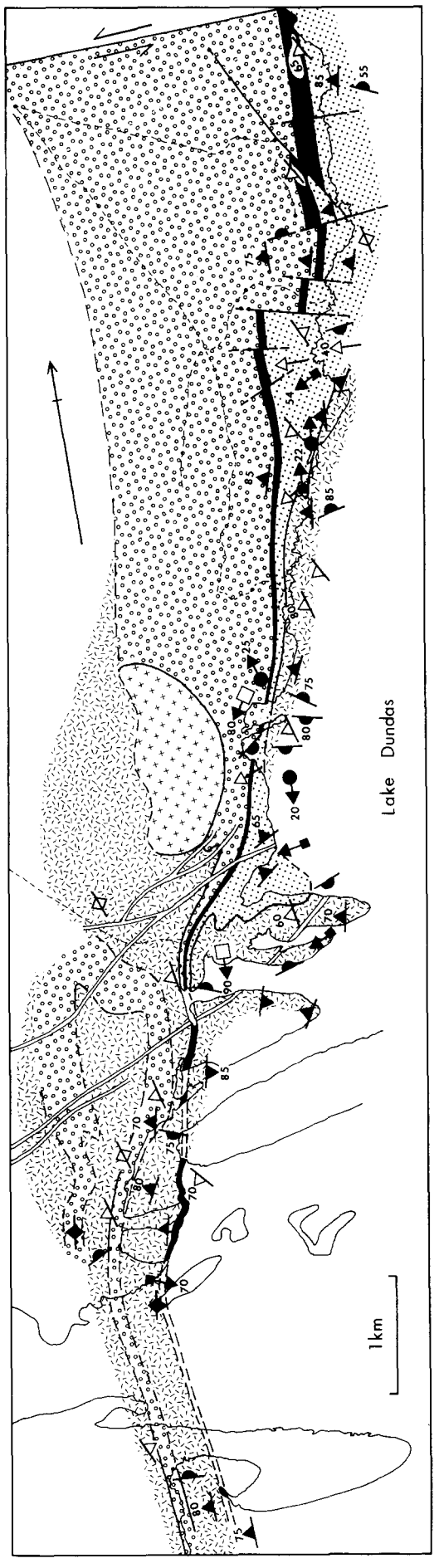

Fig. 4. Greenstone–granitoid gneiss contact relations on the western shore of Lake Dundas (see Fig. 2 for location). For clarity not all structural readings have been shown (see Fig. 6 for all data). The western greenstone–granitoid boundary is only approximate due to poor exposure.

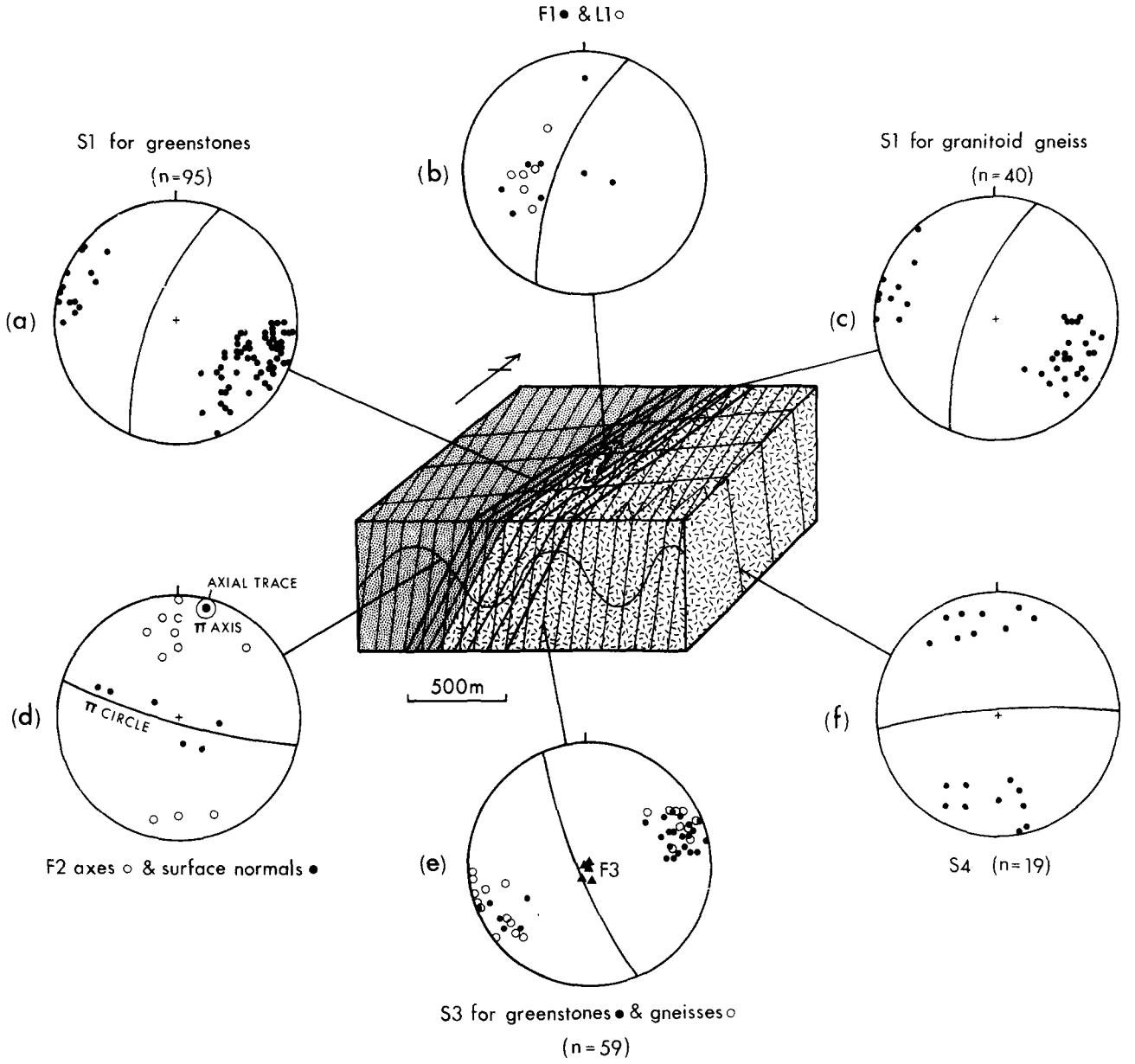

Fig. 6. Lower-hemisphere equal-area projections of structural data obtained from the study area. (a) Poles to $S1$ surfaces for greenstones (mean orientation 202°/72°NW). (b) $F1$ fold axes (mean orientation 63°/273°) and $L1$ mineral lineations (mean orientation 50°/269°) for greenstones and granitoid gneiss. (c) Poles to $S1$ surfaces for granitoid gneiss (mean orientation 202°/72°). (d) Poles (normals) to tangential surfaces used to define the $F2$ fold trend (orientation 10°/018°); $F2$ axes also shown. (e) Poles to $S3$ surfaces (mean orientation 160°/81°W) for greenstone and granitoid gneiss and $F3$ fold axes (mean orientation 86°/178°). (f) Poles to $S4$ surfaces for greenstones and granitoid gneiss (mean orientation 266°/86°N).

intrusion. Granitoids to the E show a more complex deformational history and localized anatexis. The shear zone is best developed along the E margin of the greenstones.

Structure

Figures 6(a)–(f) summarize the four main phases of deformation recognized within the study area. $D1$ structures comprise steeply dipping mylonitic, schistose or gneissose fabrics ($S1$) which have a mean orientation of 202°/72°NW for both greenstones (Fig. 6a) and granitoid gneisses (Fig. 6c). This fabric also approximates the primary strike and dip of the greenstone formations where discernible (i.e. the original bedding surface). Lying within the $S1$ planes are amphibole or mica mineral lineations ($L1$) with a mean plunge of 50°/269° and micro- to mesoscopic intrafolial folds ($F1$) with a mean plunge of 63°/273° (Fig. 6b). Most $F1$ folds possess 'Z' asymmetry (Fig. 7). More competent horizons within the shear zone (such as granitoid layers in amphibolite) show pinch-and-swell, boudinage and chocolate-tablet structures within the $S1$ surface. $D2$ is defined by upright, shallow plunging, NNE-trending mesoscopic antiforms and synforms ($F2$) which have shallow plunges and are parasitic on the Penneshaw Anticline (Fig. 6d). A weak axial planar fabric (020°/90°) was detected in places but was generally obscured by the approximately coincident orientation of $S1$. However, $F2$ folds are observed to deform the $S1$ fabric and therefore post-date it (Fig. 8). $D3$ structures coincide with the peak regional deformation and metamorphism. $S3$ is characterized by

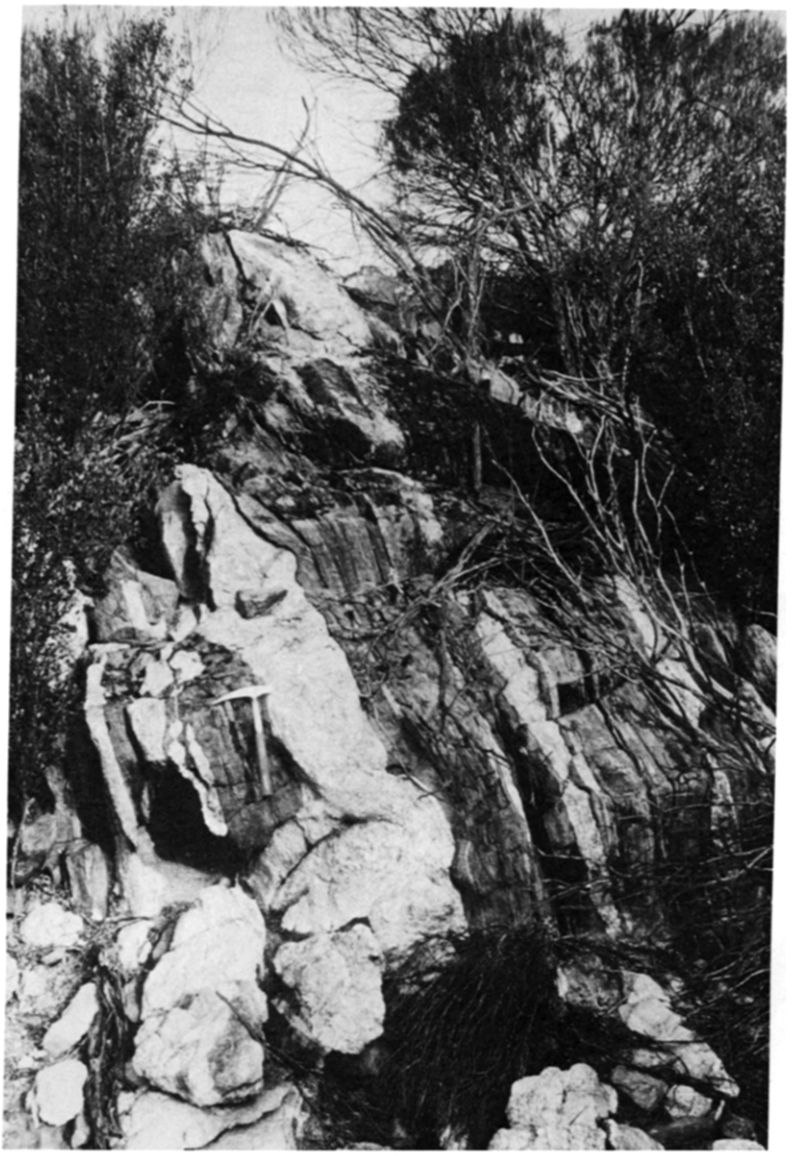

Fig. 5. Part of the highly sheared transition zone between the base of the greenstone sequence (amphibolites) and granitoid gneiss. Quartz–feldspar pegmatites locally transgress the main *S*1 fabric.

Fig. 7. *S*1 fabric developed in amphibolites of the Penneshaw Formation looking W. Note the *F*1 'Z' folds which together align to define an incipient reverse shear. Quartz–feldspar pegmatites show boudinage and pinch and swell structures. Main granitoid gneiss is located <10 m 'below' (east).

Fig. 8. Detail of *F*1 'Z' kink fold within quartzose amphibolites looking W. Kink is on limb of upright N–S trending *F*2 fold (*F*2 hinge occurs top centre of photograph). Note quartz injections on kink limbs.

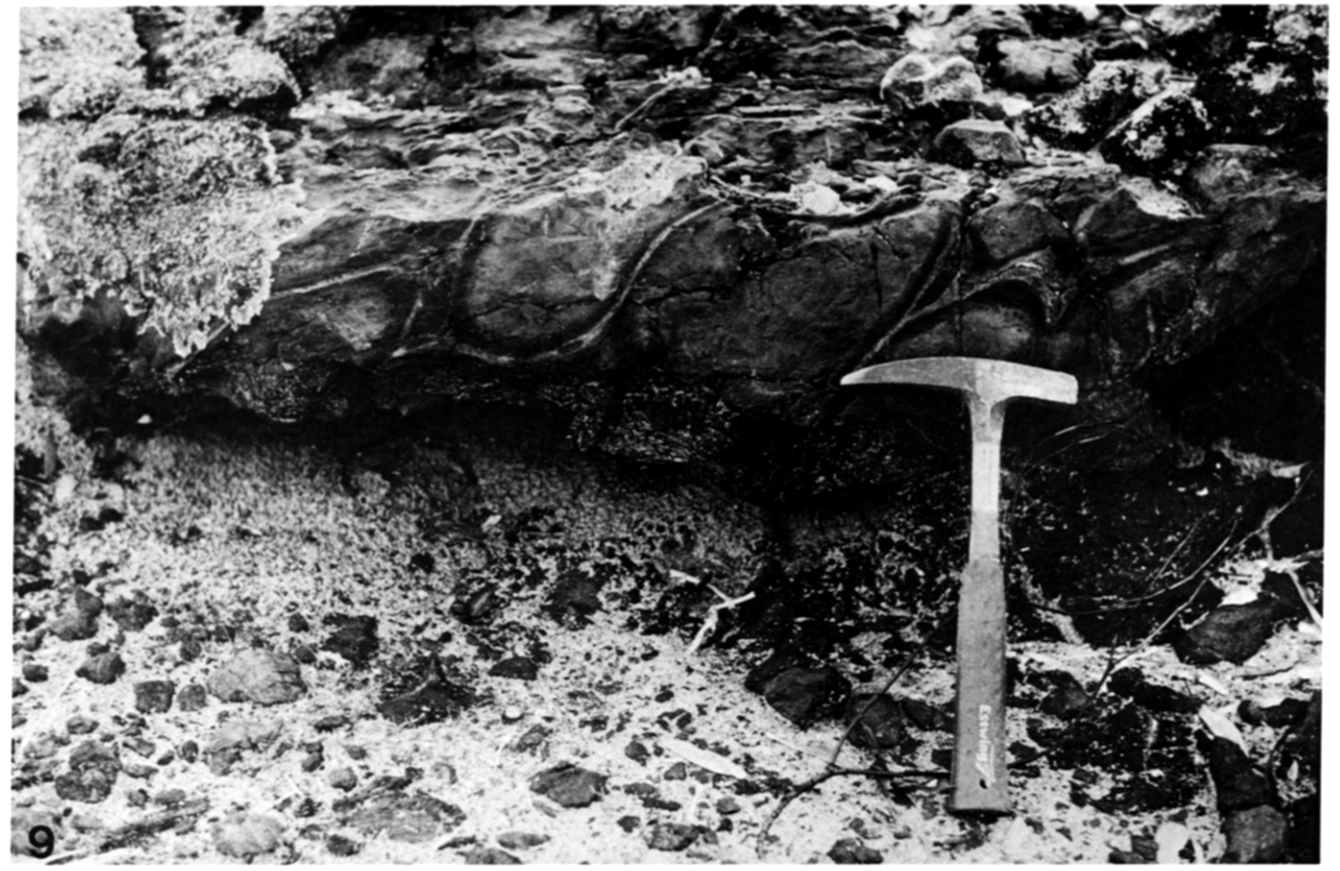

Fig. 9. Relatively undeformed metabasic pillow lavas within the basal Penneshaw Formation near the internal margin of the transition zone. Pillows young westwards (up photo) and are totally amphibolitized.

Fig. 10. Cross-section of highly deformed pillows from within the shear zone. Note how elongate they have become compared with Fig. 9. Quartzo-feldspathic material has also been introduced as veins within the $S1$ fabric and as cores to individual pillows.

Fig. 11. Cross-section of transition zone looking N. Penneshaw Formation amphibolites containing granitoid gneiss dip steeply W. Numerous anastomosing quartzo-feldspathic veins have been injected and transgress the amphibolite fabric. Note the thick gneiss layer (located below hammer) dividing into separate layers within the amphibolites.

Fig. 12. Detail of interlayered amphibolites (amphibole–plagioclase schist) and granitoid gneiss. Lower gneiss layer shows pinch and swell structure in right of photograph.

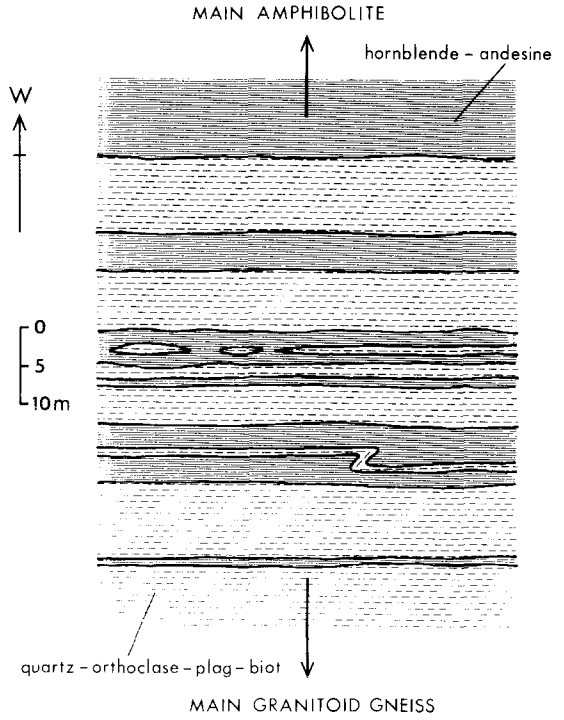

Fig. 13. Cross-section of greenstone–granitoid gneiss contact relations within a central 80 m wide section of the transition zone.

a steeply dipping NNW-trending fabric with a mean orientation of 160°/81°SW which is axial planar to subvertically plunging, close to tight *F*3 folds (Fig. 6e) and the Norseman Anticline. Interestingly, *F*3 folds in the study area were found to be steeply plunging in contrast to the supposed shallow plunge of the main Norseman Anticline (cf. Hall & Bekker 1965). *D*4 was essentially a late regional kinematic event which resulted in the formation of a steeply dipping ENE-trending fracture cleavage (*S*4), with a mean orientation of 266°/86°N, frequently associated with jointing and wrench faulting (Fig. 6f). Open, upright synforms and antiforms with axial surfaces co-planar to *S*4 and sub-horizontal plunges were also observed. The *S*4 fabric frequently hosts the Early Proterozoic intrusions of the Widgiemooltha Dyke Suite, notably the Jimberlana lopolith (Fig. 2), as well as many of the smaller doleritic dykes observed in the study area.

Several points are worth emphasizing from the structural data: firstly, while *D*2, *D*3 and *D*4 structures can be recognized on a regional scale outside the study area, *D*1 structures are of a restricted nature and are only identified close to certain greenstone–granitoid gneiss contacts. Secondly, the *D*1 structures can be demonstrated to pre-date the subsequent deformation episodes which cross-cut and/or deform *S*1. Thirdly, *S*1 approximately (but consistently) parallels the greenstone bedding surface. The central diagram of Fig. 6 summarizes these structural relationships.

The *D*1 shear zone is characterized by the lack of igneous textures and igneous mineral phases in the greenstones, although deformed pillow lava shapes can still be recognized in places (Figs. 9 and 10). Very few cross-cutting relationships between greenstones and granitoid gneiss were observed. The greenstones were never observed as intrusive at the contact and only three incidences of discordantly intrusive granitoids were observed (e.g. Fig. 11). The contact itself is not abrupt but transitional: as the granitoid gneiss is approached, concordant granitoid bands occur interleaved with the amphibolites in both increasing frequency and thickness over distances of up to *c*. 100 m. Similarly, amphibolite bands occur within the granitoid gneiss at their thickest and most frequent as the greenstone sequence is approached (Figs. 12 and 13). Lit-par-lit interleaving of granitoid material has locally produced migmatites with an *S*1 fabric which possess amphibolite melanosomes and quartz–feldspar leucosomes. This indicates that the granitoids underwent anatexis during the *D*1 shearing.

*S*1 schistose fabrics within amphibolites of the greenstones are defined by aligned amphibole grains and by alternating amphibole and plagioclase layers in amphibolite gneisses. Micas and quartz with alkali feldspar are similarly segregated in pelites. Layering in the granitoid gneisses is created by alternating ferromagnesian (biotite + amphibole) and quartz with feldspar bands.

Continuation of greenstone screens into granitoid gneiss

South of the main study area the greenstone sequence gradually thins to only a few metres width but continues on strike southwards as a steeply dipping screen within granitoid gneiss. The screen persists for at least 3 km where it is then lost due to poor exposure. The dominant lithology is banded iron formation (BIF) accompanied by amphibolite which occurs either side of the BIF or as metre wide bands separated by granitoid gneiss. Northwards, the BIF screen can be traced unbroken into the Noganyer Formation where way-up criteria within the greenstone sequence show that the stratigraphy youngs from E to W. On this criterion the E margin of the stratigraphically continuous, subvertical BIF screen is the stratigraphic base and its W margin the stratigraphic top. The screen cannot therefore be considered an isoclinally folded 'keel' within the granitoid gneiss, nor, as a sedimentary unit, can it be considered intrusive into the granitoid gneiss. Where observed the BIF screen and its upper and lower contacts with granitoid gneiss are marked by zones of high strain.

The continuation of narrow stratigraphically contiguous supracrustal screens into granitoid gneisses is a puzzling but common feature of many Archaean granitoid–greenstone terrains (e.g. Anhaeusser 1983). If the granitoid gneisses at Lake Dundas were intrusive into the greenstones it is remarkable that they have left the BIF horizon intact, especially as the gneisses, or their anatectic derivatives, were never observed to cross-cut the BIF screen. An intrusive relationship would therefore require the gneisses to have preferentially assimilated certain lithologies within the greenstones (mainly amphibolites) but left others intact (mainly BIF). Selective assimilation remains a possibility (e.g.

Table 1. Metamorphic assemblages of internal and transition zone domains. Retrograde assemblages present in the transition zone are not shown. Quartz is ubiquitous in metasediments and common in metabasites

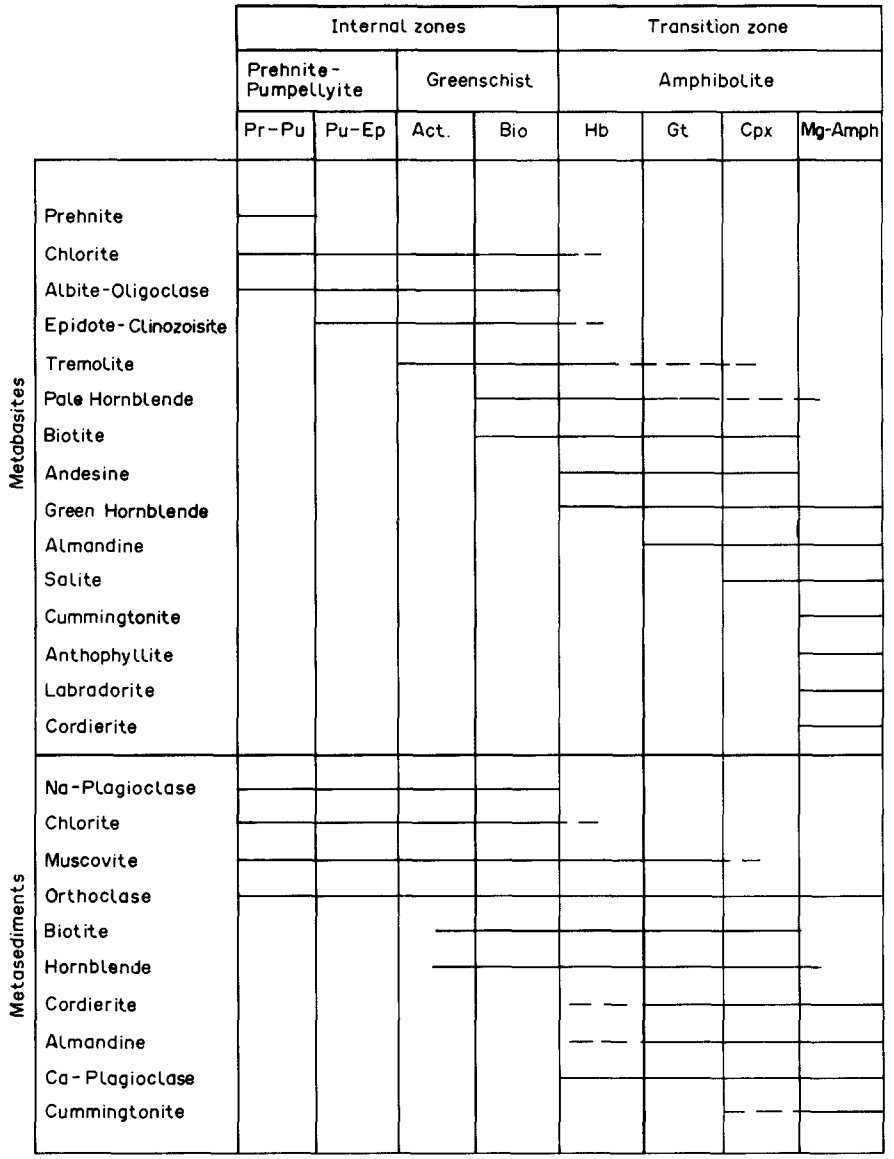

Pitcher 1970), but the highly strained nature of the BIF screen clearly indicates that there was tectonic interaction between gneiss and BIF at an early stage in the structural evolution of the greenstones.

*Pre-*D1 *structures in the polydeformed granitoid gneiss*

Whereas greenstone xenoliths commonly occur within syn- and post-RTM granitoids, especially near granitoid–greenstone contacts, none were found in the pre-RTM granitoid gneisses; the nearest candidates are thin foliated amphibolite and rare metasedimentary bands or screens (typically <2 m wide) that are up to several kilometres long. None of these screens could be traced into the greenstone sequence proper. Deformation and metamorphism preclude establishing their exact origin. The amphibolite screens may have originally been sills and dykes as possible feeders to the greenstone pile, the remnants of an earlier supracrustal sequence, or the infolded margins of the greenstone basin.

The screens are highly strained and frequently occur in sub-parallel pairs or groups only metres apart which are possibly limbs of isoclinal folds. This degree of deformation is not recorded in the main greenstone sequence indicating that these granitoid gneisses have either undergone more deformation than the greenstone sequence proper, or have had a distinct tectonic history prior to their juxtaposition with the main greenstone sequence. A good example is afforded by a large outcrop of granitoid gneiss containing amphibolite screens 2 km NE of the northern limit of the study area (Fig. 2). Most of the gneiss outcrop possesses a strong NE-trending, steeply dipping gneissosity which is coincident with neither *S*2 (NNE) nor *S*4 (ENE) fabrics. Later fabrics (*D*2–*D*4) were also observed to overprint the pre-*D*1 trend.

In view of these structural investigations Oversby's (1975, p. 1122) statement ". . . acid crustal rocks must have been present in the southern portion of the [Kalgoorlie–Norseman] area at least 3300 Ma ago. Some of

Table 2. Electron microprobe analyses of mineral phases from lithologies within the transition zone. Retrograde phases are not shown

Wt.%	1A	1B	2A	2B	3A	3B	4A	4B	5A	5B
SiO_2	54.91	52.71	55.69	49.90	47.80	56.64	43.54	51.55	51.58	37.66
TiO_2	—	—	—	—	0.60	—	0.77	—	—	—
Al_2O_3	1.32	30.16	3.03	33.74	7.69	26.88	10.47	1.12	1.50	21.20
Cr_2O_3	—	—	—	—	—	—	0.21	0.18	—	—
FeO*	21.00	0.54	17.28	3.24	20.49	0.31	22.73	14.15	33.49	33.41
MnO	0.18	—	0.14	—	0.31	—	0.32	0.32	0.35	2.78
MgO	19.40	—	21.52	11.04	9.10	—	6.32	8.83	10.60	1.65
CaO	0.69	12.98	0.30	—	11.41	9.39	11.82	23.41	0.34	4.14
Na_2O	—	4.11	—	—	0.46	6.17	1.16	—	—	—
K_2O	—	—	—	—	0.19	0.12	0.66	—	—	—
TOTAL OXIDE	97.50	100.50	97.96	97.92	98.05	99.51	98.00	99.56	97.86	100.84
FORMULA	Oxy. (23)	(8)	(23)	(18)	(23)	(8)	(23)	(6)	(23)	(24)
Si	7.92	2.38	7.83	5.03	7.15	2.56	6.68	1.99	7.89	6.03
Ti	—	—	—	—	0.07	—	0.09	—	—	—
Al	0.22	1.61	0.50	4.00	1.36	1.43	1.89	0.05	0.27	4.00
Cr	—	—	—	—	—	—	0.03	0.01	—	—
Fe*	2.53	0.02	2.03	0.27	2.56	0.01	2.92	0.46	4.29	4.47
Mn	0.02	—	0.02	—	0.04	—	0.04	0.01	0.05	0.38
Mg	4.17	—	4.51	1.66	2.03	—	1.44	0.51	2.42	0.39
Ca	0.11	0.63	0.05	—	1.83	0.45	1.94	0.97	0.06	0.71
Na	—	0.36	—	—	0.13	0.54	0.34	—	—	—
K	—	—	—	—	0.04	0.01	0.13	—	—	—
TOTAL CATION	14.97	5.00	14.94	10.96	15.21	5.00	15.50	4.00	14.98	15.98

* Total iron shown in ferrous state.
1A, Cummingtonite from cummingtonite–labradorite amphibolite (sample SC8).
1B, Labradorite plagioclase from cummingtonite–labradorite amphibolite (SC8).
2A, Anthophyllite from anthophyllite + cordierite + ilmenite + rutile assemblage (SC10).
2B, Cordierite from anthophyllite + cordierite + ilmenite + rutile assemblage (SC10).
3A, Ferro-hornblende from amphibolite schist (SC14).
3B, Andesine plagioclase from amphibolite schist (SC14).
4A, Ferro-hornblende from amphibolite schist (SC16).
4B, Salite clinopyroxene from amphibolite schist (SC16).
5A, Grunerite amphibole from banded ironstone (SC21).
5B, Almandine garnet from banded ironstone (SC21).

these older rocks may have been preserved, but have not yet been identified . . ." takes on renewed significance. If 'basement' material is present in the Norseman–Wiluna Belt then the polydeformed granitoid gneisses bordering Lake Dundas are strong candidates for the remnants of early sialic crust and as such are worthy of detailed geochronological study.

Metamorphism

In addition to being structurally distinct, the transition zone is also metamorphically anomalous when compared with the regional metamorphic grade. Greenstone lithologies within the transition zone consist of metamorphosed basalts (including metatholeiites and metakomatiitic basalts), dolerites and gabbros, pelites, banded iron-formation and ultramafics. Table 1 summarizes the occurrence of metamorphic phases within the transition zone. The effects of contact metamorphism due to basic, ultrabasic and granitoid intrusion are excluded from the table. Metabasites in the transition zone are represented by hornblende–plagioclase assemblages with or without quartz and accessory sphene, apatite, pyrite and ilmenite. Hornblende + andesine marks the threshold of the amphibolite facies and is the lowest grade recognized. At progressively higher grades almandine, salite, cummingtonite and anthophyllite appear concomitant with an increase in anorthite content in plagioclase. Cummingtonite + labradorite and anthophyllite + cordierite represent the highest-grade assemblages found in the transition zone (Table 1). The former is considered to form in basites by the reaction tschermakite + SiO_2 = cummingtonite + anorthite + H_2O with a rise in temperature corresponding to the change from mid- to high amphibolite facies (e.g. Shido 1958). Ultramafic flows have been partly serpentinized, otherwise olivine + talc + tremolite + chlorite + carbonate + anthophyllite + orthopyroxene assemblages are developed, comparable to those described by Willett *et al.* (1978).

Iron-formations within the transition zone typically comprise quartz + haematite + grunerite + almandine and correspond to the high grade assemblages described by Gole (1981). Pelitic metasediments are dominated by quartz + feldspar + mica assemblages with additional chlorite, cordierite, hornblende or almandine. A selection of electron microprobe analyses of various mineral phases from within the transition zone are shown in Table 2.

Most of the transition zone lithologies show retrogressive overprinting to the greenschist and lower facies and this frequently inhibits the identification of feldspars which are invariably pseudomorphed by saussurite. Retrograde epidote, albite, chlorite and muscovite are

Table 3. Summary of the structural and metamorphic evolution of the Norseman region

		Effect	Inferred heat source	Facies	Style	Age (Ga)
Archaean	Internal	Pervasive oceanic hydrothermal metamorphism	Submarine extrusive and high-level intrusive magmas	Up to greenschist	Static	2.7–?3.3
		Contact metamorphism	Basic and ultrabasic sills, dykes and cupolas (magma chambers)	Up to amphibolite	Static	
	External	Localized dynamothermal metamorphism	Shear heating between tectonically juxtaposed greenstones and granitoid gneiss	Up to amphibolite	Dynamic ($D1$)	
		Regional metamorphism and tectonism plus contact metamorphism	Burial plus syn-RTM granitoid intrusion	Regional metamorphism mainly up to greenschist. Contact aureoles up to amphibolite	Dynamic ($D2 \rightarrow D4$)	2.6–2.7
		Contact metamorphism	Granitoid intrusions	Locally up to amphibolite	Static (post-RTM)	
Proterozoic		Contact metamorphism	Jimberlana lopolith and related dyke suite	Locally up to amphibolite	Static	2.4
		Regional metamorphism and tectonism	Fraser orogeny	Up to granulite 30 km SE of Norseman	Dynamic	1.2–1.9

also common but can be distinguished from the amphibolite facies assemblages by their random orientation or by their cross-cutting relationships due to later deformation.

Aside from pre-, syn- and post-RTM granitoid–greenstone contacts, the internal zones of the greenstone sequence are in the prehnite–pumpellyite, greenschist and low amphibolite (epidote–amphibolite) facies. Greenschist to low amphibolite facies grades were reached during the development of the regional $S3$ cleavage and in this respect the internal zones are not truly 'static' (cf. Binns *et al.* 1976). The internal zones are largely characterized by hydrothermal and retrogressive overprinting of igneous and sedimentary assemblages. Disequilibrium metamorphic textures predominate and igneous fabrics tend to survive. In the mafic lithologies pyroxenes are partially or completely replaced by amphibole and calcic plagioclases are typically found saussuritized to epidote + clinozoisite + albite assemblages; both may persist, at least in outline, as porphyroclasts. The metamorphic phases present in the lower grade–lower strain internal zones of the greenstones are shown in Table 1. A more detailed account of greenstone metamorphism will be presented elsewhere.

Table 3 attempts to place the transition zone in context within the overall structural and metamorphic evolution of the Norseman granitoid–greenstone terrain. Low grade hydrothermal alteration of the greenstone pile under essentially static conditions is attributed to pervasive hot rock–water interaction occurring in the vicinity of subaqueous eruptive centres and high level intrusives. The presence of pillow lavas unequivocally testifies to the subaqueous eruption of these magmas (Fig. 9). Higher grades of contact metamorphism were locally reached at the contracts around basic and ultrabasic sills, dykes and magma chambers. Both these effects are the direct result of heat generated during constructive greenstone igneous activity and are consequently referred to as 'internal' metamorphic processes. These events were succeeded by thermal influences from external sources including shear heating along faults during tectonic juxtapositioning of the greenstone pile with granitoid gneiss, granitoid intrusion (involving syn- and post-RTM variants) and burial and deformation during the main kinematic event. It is clear that the Norseman greenstone sequence must have been buried following tectonic juxtaposition with the granitoid gneisses because coarse-grained plutonic granitoids occur as discordant intrusions within supracrustal basic volcanics and sediments. However, it is not clear how burial was achieved: successive constructive igneous episodes or tectonic stacking could have thickened the greenstone pile such that it could host plutonic intrusions. No high pressure mineral phases were identified during the investigation so it is unlikely that the base of the greenstone pile was depressed to depths in excess of the maximum apparent stratigraphic thickness of 25 km (*c.* 8 kb).

Subsequent metamorphic events involve contact effects from the Early Proterozoic giant lopolith–minor dyke intrusions and the Mid-Proterozoic Albany–Fraser orogeny which, although resulting in the reworking of the Archaean shield into a polydeformed granulite facies terrain, occurs at some distance from the Norseman region (Table 3).

DISCUSSION

Origin of the pre-RTM contact

Previous workers have attributed the formation of dynamic-style domains within the greenstones of the Eastern Yilgarn Block to the proximity of syn-RTM granitoid gneiss diapirs which penetrated greenstone sequences during remobilization of a sialic substratum (Binns *et al.* 1976, Archibald & Bettenay 1977, Archibald *et al.* 1978). There is evidence that this occurred in the Norseman area, not only around the Wid-

giemooltha and Pioneer Domes, where Archibald and co-workers gathered much of their data, but also from the Goodia Dome, a SE-trending continuation of these syn-RTM structures which, at both ground and satellite levels, can be observed to truncate the Mount Kirk Syncline (Fig. 2). (Spray & Burgess 1984). However, this interpretation does not adequately account for the granitoid–greenstone relations exposed on the western shores of Lake Dundas for the following reasons:

(1) The granitoid gneiss possesses structural fabrics which can be demonstrated to pre-date the $D1$–$D4$ events. These pre-$D1$ structures were not observed in the greenstones.

(2) In contrast to the syn- and post-RTM granitoids, no low strain rounded or angular xenoliths were found in these granitoid gneisses. Only high strain bands and screens of amphibolite and occasional metasediment occur. These are always found highly tectonized, frequently isoclinally folded and boudinaged and as such are more deformed than any of the lithologies observed within the main greenstone sequence.

(3) The $D1$ structures developed in the greenstone–granitoid gneiss contact are indicative of high strain and comprise isoclinal folds with sub-vertical plunges. The orientation of $F1$ folds is inconsistent with an origin by granitoid intrusion and updoming whereby folds possessing subhorizontal plunges would be generated.

(4) The presence of planar fabrics, pinch-and-swell, boudinage, chocolate-tablet and complex fold structures generally indicates a tectonic rather than an intrusive origin.

(5) The continuation of unbroken screens of highly strained attenuated greenstone sequence into the granitoid gneiss for several kilometres also indicates a tectonic rather than an intrusive origin.

(6) The greenstone–granitoid gneiss contact occurs sub-parallel to the greenstone bedding surface for a distance of over 30 km. No major discordant granitoid intrusions or stratigraphic disruption of the greenstones were detected over this distance. Such concordance is incompatible with vertical granitoid diapirism.

The above evidence favours a purely tectonic origin for the $D1$ event. In addition, the removal of subsequent folding episodes (effectively only the upright $F2$ folding event) reveals that the $S1$ surface was originally shallow dipping. Although the high grade–high strain western contact is largely obscured by later syn- and post-RTM intrusions, the greenstone screens within the gneiss immediately S of the study area indicate that both the stratigraphic top and base of the greenstone intercalations were zones of tectonic movement. Thus, there is limited evidence that pre-RTM granitoid gneiss was also thrust over the greenstone pile during $D1$ such that a gneiss–greenstone–gneiss tectonic sandwich was created. Irrespective of the age constraints, the structural data show that the subhorizontal movements occurred prior to regional metamorphism and magmatism. An important objective would be to determine the extent of greenstone transport. If the greenstones are virtually autochthonous (or parautochthonous) the presence of the pre-$D1$ structures in certain gneisses provides unequivocal evidence, on structural grounds alone, that the gneisses are older than the greenstones and that they constitute the remains of the basement to the supracrustal sequence. If, however, the greenstones are allochthonous then the pre-$D1$ granitoid fabric merely indicates a more complex deformation history for these granitoids, but not one that necessarily pre-dates greenstone formation, nor does it reveal whether these gneisses are the remnants of early basement.

Other examples of subhorizontal tectonics from granitoid–greenstone terrains

There is growing evidence that many Archaean granitoid–greenstone terrains have undergone a degree of horizontal interaction at some stage during their evolution. In their summary of the Kambalda area geology to the N of Norseman, Gresham & Loftus-Hills (1981) recognized an early ($D1$) phase of deformation characterized by tight to isoclinal, recumbent folds associated with thrusts. Similarly, Archibald *et al.* (1978, 1981) described localized recumbent $F1$ folds from the area W and S of Kambalda. Early recumbent folds and a related flat-lying schistosity have also been identified in the Agnew supracrustal belt 400 km N of Kalgoorlie (Platt *et al.* 1978, Platt 1980). In the Pilbara Block of Western Australia (Fig. 1), Hickman & Lipple (1975) and Bickle *et al.* (1980) described greenstone intercalations within the granitoid gneiss of the Shaw Batholith which can be traced into the surrounding greenstone sequence. The intercalations mark high strain–high grade zones and their structure is consistent with the thrusting of granitoid gneiss over greenstones followed by recumbent folding.

Stowe (1974), in his investigations of the Archaean greenstones and granitoids in Zimbabwe, recognized a number of phyllonitic and mylonitic shear zones within and at the base of the Selukwe Schist Belt which he concluded were a remnant of a large recumbent greenstone nappe. At its base a 500 m wide shear zone was identified separating the allochthonous greenstone sequence from gneissic basement. 300 km to the WSW, Smith & Fripp (1973) described a gneissose and migmatitic transition zone between the Matapos granitoid and the Bulawayo greenstone belt. The transition comprises highly schistose amphibolites interleaved with gneissose granitoids. They concluded that the greenstone margin was sheared prior to the introduction of the main body of granitoid and their description of the contact suggests that it involved tectonic interaction between the greenstones and granitoid gneiss. Coward *et al.* (1976) recognized a deformation phase that preceded regional cleavage formation in the Limpopo belt of Botswana and western Zimbabwe in form of recumbent isoclinal folds which created allochthonous greenstone nappes. In the Motjane Schist Belt of Swaziland, Jackson & Robertson (1983) identified early recumbent and reclined isoclinal folds within the Onverwacht metabasites which they interpreted to indicate a period

of horizontal translation, possibly in a thrust or nappe regime. Recent work in the Barberton Mountain Land of southern Africa has also revealed the presence of recumbent folds, inverted stratigraphy, stratigraphic repetition, thrusts and olistostromes within the greenstone sequence (De Wit 1982, De Wit *et al.* 1983).

As in the Norseman region, all these examples show that subhorizontal tectonics occurred relatively early in the evolution of the respective Archaean terrain and prior to any ensuing vertical tectonics and associated granitoid diapirism.

The heat source

The source of heat for the dynamothermal event recorded on the western shore of Lake Dundas is a matter for debate. Simple burial is discounted because the change in metamorphic grade in passing from unsheared to sheared domains is considered too abrupt to be explained by the prevailing geothermal gradient, even allowing for the possible existence of a steeper gradient in the Archaean. The three most likely heat sources are (1) thrusting a hot immature greenstone sequence onto a granitoid basement, (2) thrusting a relatively cold greenstone sequence onto a hot granitoid basement or (3) shear heating along the plane of contact.

The first and third options are analogous to conditions prevailing at the base of certain Phanerozoic ophiolites: their early tectonic displacement also results in the formation of high grade dynamothermal contacts <1 km thick (Spray 1984). However, rather than comprising a mantle unit underlying a thin crustal sequence, as do intact ophiolites and Phanerozoic oceanic lithosphere, most Archaean greenstones consist of a thick volcanic pile interspersed with sedimentary horizons intruded by basic and ultrabasic sills and dykes. To what extent these apparent differences reflect a genuine contrast between the two types of ultramafic–mafic complex is a matter of contention. However, in the case of the Norseman greenstone sequence, both pillow lavas and sedimentary horizons occur close to its stratigraphic base and this obviates the possibility of hot upper mantle peridotite being the heat source for the contact metamorphism (Figs. 9 and 10). The Norseman greenstone sequence is wholly of a crustal nature and no distinct mantle unit was identified within it. Whether or not it was originally attached to a mantle unit is not known.

It is possible that hot granitoid was the heat source, but not in a purely intrusive form because the structural evidence clearly supports a thrust relationship. Thrusting supracrustals onto hot granitoid is considered unlikely because it would have occurred at relatively high levels if not under submarine or subaerial conditions, clearly an unsuitable setting for significant granitoid heat retention in order to produce plutonic textures or for the transfer of heat from hot granitoids to greenstones.

Shear heating is considered the most viable source of heat for generating the dynamothermal transition zone. This could have occurred during greenstone overthrusting provided that shear stresses and fault velocities were sufficiently high (Scholtz 1980). Shear stresses of *c.* 1 kb are required at present plate tectonic rates in order to generate heat by friction at shallow depths or by plastic deformation in deeper ductile shear zones. Alternatively, shear stresses substantially less than 1 kb would be sufficient if fault velocities attained several tens of cms per year, a situation consistent with more rapid plate movements in the Archaean (Sleep & Windley 1982). Significantly, because of the presence of granitoid within the Lake Dundas transition zone, the effects of shear heating would have been buffered by the melting of granite at *c.* 650°C and this is compatible with the attainment of upper amphibolite facies grade in the adjacent greenstone lithologies. Furthermore, because the granitoid–greenstone shear zone represents an interface between rock types of contrasting ductility it could have facilitated the localized production of melts (Fleitout & Froidevaux 1980). Shear heating in a stratified system can induce higher temperatures in the harder more competent material, in this case granitoid, which, due to it having a lower melting point than the adjacent amphibolites, could have undergone limited anatexis. It is by this process that granitoid intercalations are considered to have been introduced into the greenstones during the $D1$ shearing as melts were injected away from the initial granitoid–greenstone interface.

CONCLUSIONS

The dynamothermal transition zone between Archaean greenstone and granitoid gneiss at Lake Dundas is considered to have evolved as a subhorizontal shear zone during the overthrusting of greenstones onto granitoid gneiss during the early stages of the evolution of the Norseman granitoid–greenstone terrain. Granitoid gneiss may have also been thrust over the greenstones. Provided that Archaean 'plate' movements were more rapid than at present, a view consistent with the proposed lower viscosity of Archaean mantle and its higher heat flow, shear heating would have been a viable cause of metamorphism within the contact zone and may in general have been a more important heat source during the Archaean than in Proterozoic or Phanerozoic times. The formation of a dynamic-style domain by this process does not preclude the possibility of creating similar zones by later syn-RTM granitoid intrusion, but provides an explanation for the occurrence of high strain–high grade greenstone margins adjacent to demonstrably pre-RTM granitoid gneiss.

An origin by overthrusting indicates that the greenstone sequence at Norseman has undergone a degree of tectonic transport, the extent of which is presently unknown, and that internally it may be tectonically stacked to its present apparent total thickness of 24 km. Tectonic discontinuities within the Norseman stratigraphy have yet to be identified. Future stratigraphic investigations within the Norseman greenstones should include searches for shear zones (now possibly quartz

injected and mineralized), repetition, inversion and truncation of the stratigraphy and zones of anomalous metamorphic grade.

Acknowledgements—This work was completed during tenure of an Earth Sciences Research Fellowship from King's College, Cambridge (U.K.) in collaboration with the Western Mining Corporation Ltd (Australia). Logistical support was provided by W.M.C., King's College and the Royal Society. I thank Geoff Hopkins, Richard Keele and Pat MacGeehan for helpful discussions during field excursions in the area, Roy Woodall for his continued support and my wife Alison for field assistance. Simon Lamb, Nigel Woodcock and other colleagues in the Department of Earth Sciences at Cambridge kindly made constructive comments on the manuscript. Cambridge Earth Sciences contribution 500.

REFERENCES

Anhaeusser, C. R. 1983. The geology of the Schapenburg greenstone remnant and surrounding Archaean granitic terrane south of Badplaas, Eastern Transvaal. *Spec. Publs geol. Soc. Afr.* **9**, 31–44.

Archibald, N. J. & Bettenay, L. F. 1977. Indirect evidence for tectonic reactivation of a pre-greenstone sialic basement in Western Australia. *Earth Planet. Sci. Lett.* **33**, 370–378.

Archibald, N. J., Bettenay, L. F., Bickle, M. J. & Groves, D. I. 1981. Evolution of Archaean crust in the Eastern Goldfields Province of the Yilgarn Block, Western Australia. *Spec. Publs geol. Soc. Aust.* **7**, 491–504.

Archibald, N. J., Bettenay, L. F., Binns, R. A., Groves, D. I. & Gunthorpe, R. J. 1978. The evolution of Archaean greenstone terrains, Eastern Goldfields Province, Western Australia. *Precambrian Res.* **6**, 103–131.

Arriens, P. A. & Lambert, I. B. 1969. On the age and strontium isotopic geochemistry of granulite facies rocks from the Fraser Range, Western Australia and the Musgrave Ranges, Central Australia. *Spec. Publs geol. Soc. Aust.* **2**, 377–388.

Bickle, M. J., Bettenay, L. F., Boulter, C. A., Groves, D. I. & Morant, P. 1980. Horizontal tectonic interaction of an Archaean gneiss belt and greenstones, Pilbara Block, Western Australia. *Geology* **8**, 525–529.

Binns, R. A., Gunthorpe, R. J. & Groves, D. I. 1976. Metamorphic patterns and development of greenstone belts in the Eastern Yilgarn Block, Western Australia. In: *The Early History of the Earth* (edited by Windley, B. F.). Wiley, New York, 303–313.

Campbell, I. H., McCall, G. J. H. & Tyrwhitt, D. S. 1970. The Jimberlana Norite, Western Australia—a smaller analogue of the Great Dyke of Rhodesia. *Geol. Mag.* **107**, 1–12.

Claoue-Long, J. C., Thirlwall, M. F. & Nesbitt, R. W. 1984. Revised Sm–Nd systematics of Kambalda greenstones, Western Australia. *Nature, Lond.* **307**, 697–701.

Compston, W. & Arriens, P. A. 1968. The Precambrian geology of Australia. *Can. J. Earth Sci.* **5**, 561–583.

Coward, M. P., Lintern, B. C. & Wright, L. I. 1976. The pre-cleavage deformation of the sediments and gneisses of the northern part of the Limpopo belt. In: *The Early History of the Earth* (edited by Windley, B. F.). Wiley, New York, 323–330.

De Wit, M. J. 1982. Gliding and overthrust nappe tectonics in the Barberton Greenstone Belt. *J. Struct. Geol.* **4**, 117–136.

De Wit, M. J., Fripp, R. E. P. & Stanistreet, I. G. 1983. Tectonic and stratigraphic implications of new field observations along the southern part of the Barberton Greenstone Belt. *Spec. Publs geol. Soc. Afr.* **9**, 21–29.

Doepel, J. J. G. 1973. *Norseman W.A.* Western Australia Geol. Survey 1 : 50 000 Series with explanatory notes.

Ellis, H. A. 1953. Norseman Gold Mines. In: *Geology of Australian Ore Deposits. 5th Empire Min. Metall. Congr. Aust. New Zealand* (edited by Edwards, A. B.). **1**, 150–158.

Fleitout, L. & Froidevaux, C. 1980. Thermal and mechanical evolution of shear zones. *J. Struct. Geol.* **2**, 159–164.

Gee, R. D. 1979. Structure and tectonic style of the Western Australian shield. *Tectonophysics* **58**, 327–367.

Gee, R. D., Baxter, J. L., Wilde, S. A. & Williams, I. R. 1981. Crustal development in the Archaean Yilgarn Block, Western Australia. *Spec. Publs geol. Soc. Aust.* **7**, 43–56.

Gemuts, I. & Theron, A. 1975. The Archaean between Coolgardie and Norseman—stratigraphy and mineralization. In: *Economic Geology of Australia and Papua New Guinea—1 Metals* (edited by Knight, C. L.) *Aust. Inst. Min & Met. Monogr.* **5**, 66–74.

Gole, M. J. 1981. Archaean banded iron-formations, Yilgarn Block, Western Australia. *Econ. Geol.* **76**, 1954–1974.

Gresham, J. J. & Loftus-Hills, G. D. 1981. The geology of the Kambalda Nickel Field, Western Australia. *Econ. Geol.* **76**, 1373–1416.

Hall, H. I. E. & Bekker, C. 1965. Gold deposits of Norseman. *Comm. Min. Met. Australia New Zealand Congr.* **8**, 101–106.

Hickman, A. H. & Lipple, S. L. 1975. *Marble Bar W.A.* Western Australia Geol. Survey 1 : 250 000 Series with explanatory notes.

Jackson, M. P. A. & Robertson, D. I. 1983. Regional implications of Early Precambrian strains in the Onverwacht Group adjacent to the Lochiel Granite, North-West Swaziland. *Spec. Publs geol. Soc. South Afr.* **9**, 45–62.

Lovering, J. F., Travis, G. A., Comaford, D. J. & Kelly, P. R. 1981. Evolution of the Gondwana Archaean shield: zircon dating by ion microprobe, and relationships between Australia and Wilkes Land (Antarctica). *Spec. Publs geol. Soc. Aust.* **7**, 193–203.

McCulloch, M. T. & Compston, W. 1981. Sm–Nd age of Kambalda and Kanowna greenstones and heterogeneity in the Archaean mantle. *Nature, Lond.* **294**, 322–327.

McCulloch, M. T., Compston, W. & Froude, D. 1983. Sm–Nd and Rb–Sr dating of Archaean gneisses, Eastern Yilgarn Block, Western Australia. *J. geol. Soc. Aust.* **30**, 149–153.

Oversby, V. M. 1975. Lead isotopic systematics and ages of Archaean acid intrusives in the Kalgoorlie–Norseman area, Western Australia. *Geochim. cosmochim. Acta* **40**, 817–829.

Pitcher, W. S. 1970. Ghost stratigraphy in intrusive granites: a review. In: *Mechanisms of Igneous Intrusion* (edited by Newell, G. & Rast, N.). Spec. Issue *Geol. J.* **2**, 123–140.

Platt, J. P. 1980. Archaean greenstone belts: a structural test of tectonic hypotheses. *Tectonophysics* **65**, 127–150.

Platt, J. P., Allchurch, P. D. & Rutland, R. W. R. 1978. Archaean tectonics in the Agnew supracrustal belt, Western Australia. *Precambrian Res.* **7**, 3–30.

Roddick, J. C. 1984. Emplacement and metamorphism of Archaean mafic volcanics at Kambalda, Western Australia—geochemical and isotopic constraints. *Geochim. cosmochim. Acta* **48**, 1305–1318.

Scholz, C. H. 1981. Shear heating and the state of stress on faults. *J. geophys. Res.* **85**, 6174–6184.

Shido, F. 1958. Plutonic and metamorphic rocks of the Nakoso and Oritono districts in the central Abukuna Plateau. *J. Fac. Sci. Tokyo* **11**, 131–217.

Sleep, N. H. & Windley, B. F. 1982. Archaean plate tectonics: constraints and inferences. *J. Geol.* **90**, 363–379.

Smith, C. C. & Fripp, R. E. P. 1973. The northern contact facies of the Matapos Granite, Rhodesia. *Spec. Publs geol. Soc. Afr.* **3**, 447–453.

Sofoulis, J. 1963. *Widgiemooltha W.A.* Western Australian Geol. Survey 1 : 250 000 Series with explanatory notes.

Spray, J. G. 1984. Possible causes and consequences of upper mantle decoupling and ophiolite displacement. *Spec. Publs geol. Soc. Lond.* **13**, 255–268.

Spray, J. G. & Burgess, L. A. 1984. Geological interpretation of Landsat images from the Norseman region, Western Australia. Western Mining Corporation Internal Report K/2834, Kalgoorlie, Western Australia.

Stowe, C. W. 1974. Alpine-type structures in the Rhodesian basement complex at Selukwe. *J. geol. Soc. Lond.* **130**, 411–425.

Turek, A. 1966. Rb–Sr isotopic studies in the Kalgoorlie–Norseman area, Western Australia. Unpublished Ph.D. thesis, Australian National University.

Willett, G., Eshuys, E. & Guy, B. 1978. Ultramafic rocks of the Widgiemooltha–Norseman area, Western Australia: petrological diversity, geochemistry and mineralization. *Precambrian Res.* **6**, 133–156.